

Nuclear constraints on the inner edge of neutron star crusts

Lie-Wen Chen^{a *}, Bao-An Li^{b †}, Hong-Ru Ma^a, and Jun Xu^{a ‡}

^aDepartment of Physics, Shanghai Jiao Tong University, Shanghai 200240, China

^bDepartment of Physics and Astronomy, Texas A&M University-Commerce, Commerce, Texas 75429-3011, USA

We show that the widely used parabolic approximation to the Equation of State (EOS) of asymmetric nuclear matter leads systematically to significantly higher core-crust transition densities and pressures. Using an EOS for neutron-rich nuclear matter constrained by the isospin diffusion data from heavy-ion reactions in the same sub-saturation density range as the neutron star crust, the density and pressure at the inner edge separating the liquid core from the solid crust of neutron stars are determined to be $0.040 \text{ fm}^{-3} \leq \rho_t \leq 0.065 \text{ fm}^{-3}$ and $0.01 \text{ MeV/fm}^3 \leq P_t \leq 0.26 \text{ MeV/fm}^3$, respectively. Implications of these constraints on the Vela pulsar are discussed.

1. INTRODUCTION

The inner crust in neutron stars spans the region from the neutron drip-out point to the inner edge separating the solid crust from the homogeneous liquid core and plays an important role in understanding many astrophysical observations [1, 2, 3]. While the neutron drip-out density ρ_{out} is relatively well determined to be about $4 \times 10^{11} \text{ g/cm}^3$ [4], the transition density ρ_t at the inner edge is still largely uncertain mainly because of our very limited knowledge on the EOS of neutron-rich nucleonic matter, especially the density dependence of the nuclear symmetry energy $E_{sym}(\rho)$ [2].

Recently, significant progress has been made in constraining the EOS of neutron-rich nuclear matter using terrestrial laboratory experiments (See, e.g., Ref. [5] for the most recent review). In particular, the analysis of isospin-diffusion data [6, 7, 8] in heavy-ion collisions has constrained tightly the $E_{sym}(\rho)$ in exactly the same sub-saturation density region around the expected inner edge of neutron star crust. In the present talk, we report our recent work on locating the inner edge of the neutron star crust using terrestrial nuclear laboratory data within both thermodynamical and dynamical methods [9].

*Supported in part by the NNSF of China under Grant No. 10575071, 10675082 and 10975097, Shanghai Rising-Star Program under Grant No.06QA14024, and the National Basic Research Program of China (973 Program) under Contract No.2007CB815004.

†Supported in part by the US NSF under Grants No. PHY0652548 and No. PHY0757839, the Texas Coordinating Board of Higher Education ARP grant No. 003565-0004-2007 and the Research Corporation Grant No. 7123.

‡Current address: Cyclotron Institute and Physics Department, Texas A&M University, College Station, Texas 77843-3366, USA

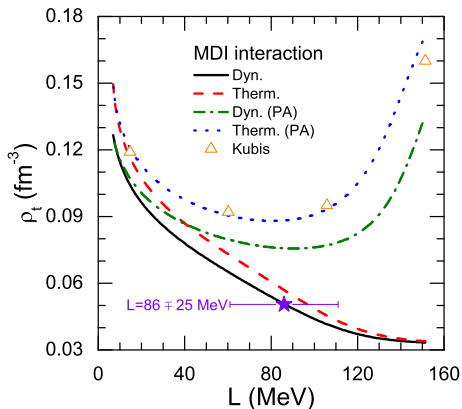


Figure 1. (Color online) The ρ_t versus L from the dynamical and thermodynamical methods with and without the PA using the MDI interaction. The triangles are obtained by Kubis [11] and the star with error bar represents $L = 86 \pm 25$ MeV. Taken from Ref. [9]

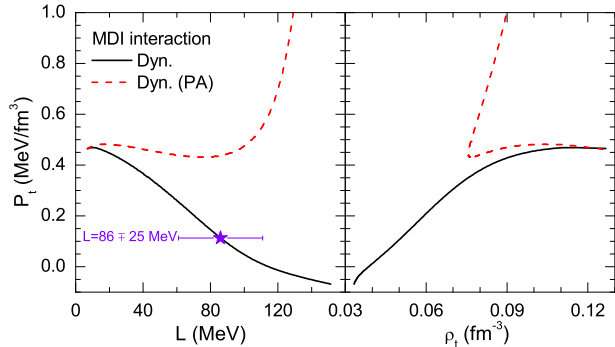


Figure 2. (Color online) The P_t versus L and ρ_t by using the dynamical method with and without the PA using the MDI interaction. The star with error bar in the left panel represents $L = 86 \pm 25$ MeV. Taken from Ref. [9]

2. RESULTS

Shown in Fig. 1 is the ρ_t as a function of the slope parameter of the symmetry energy $L = 3\rho_0 \frac{\partial E_{sym}(\rho)}{\partial \rho} \Big|_{\rho=\rho_0}$ with the MDI interaction [10]. For comparisons, we have included results using both the dynamical and thermodynamical methods with the full EOS and its parabolic approximation (PA), i.e., $E(\rho, \delta) = E(\rho, \delta = 0) + E_{sym}(\rho)\delta^2 + O(\delta^4)$ using the same MDI interaction. The thermodynamical method is the long wave length limit of the dynamical one when the Coloumb and surface interactions are neglected [9]. With the full MDI EOS, it is clearly seen that the ρ_t decreases almost linearly with increasing L within both methods. It is interesting to see that the two methods give very similar results (the difference is actually less than 0.01 fm^{-3}). Surprisingly, the PA drastically changes the results, especially for stiffer symmetry energies (larger L values). Also included in Fig. 1 are the predictions by Kubis using the PA of the MDI EOS in the thermodynamical approach [11]. The large error introduced by the PA is understandable since the β -stable npe matter is usually highly neutron-rich, thus the contribution from the higher order terms in δ is appreciable. This is especially true for the stiffer symmetry energy which generally leads to a more neutron-rich npe matter at subsaturation densities. In addition, simply because of the energy curvatures involved in the stability conditions, the contributions from higher order terms in the EOS are multiplied by a larger factor than the quadratic term. Our results indicate that one may introduce a huge error by assuming *a priori* that the EOS is parabolic with respect to the isospin asymmetry for a given interaction in calculating the ρ_t . We thus apply the experimentally constrained L to the $\rho_t - L$ correlation obtained using the full EOS in constraining the ρ_t in the dynamical method as it is more complete and realistic. As shown in Fig. 1, the constrained

$L = 86 \pm 25$ MeV obtained from the transport model analysis of the isospin diffusion data [6, 7, 8] then limits the transition density to $0.040 \text{ fm}^{-3} \leq \rho_t \leq 0.065 \text{ fm}^{-3}$.

The pressure at the inner edge, P_t , is also an important quantity which might be measurable indirectly from observations of pulsar glitches [2, 3]. Shown in Fig. 2 is the P_t versus L and ρ_t . Again, it is seen that the PA leads to huge errors for larger (smaller) L (ρ_t) values. For the full MDI EOS, the P_t decreases (increases) with the increasing L (ρ_t) while it displays a complex relation with L or ρ_t for the PA. The complex behaviors are due to the fact that the ρ_t does not vary monotonically with L for the PA as shown in Fig. 1. From the constrained L values, the P_t is limited between 0.01 MeV/fm^3 and 0.26 MeV/fm^3 .

The constrained values of ρ_t and P_t have important implications on many properties of neutron stars [1, 2, 3]. As it was shown in Ref. [2], the crustal fraction of the total moment of inertia of a neutron star, i.e., $\Delta I/I$ depends sensitively on the P_t and ρ_t at subsaturation densities, but there is no explicit dependence upon the higher-density EOS. So far, the only known limit of $\Delta I/I > 0.014$ was extracted from studying the glitches of the Vela pulsar [3]. This together with the upper bounds on the P_t and ρ_t ($\rho_t = 0.065 \text{ fm}^{-3}$ and $P_t = 0.26 \text{ MeV/fm}^3$) sets approximately a minimum radius of $R \geq 4.7 + 4.0M/M_\odot$ km for the Vela pulsar. The radius of the Vela pulsar is predicted to exceed 10.5 km should it have a mass of $1.4M_\odot$. A more restrictive constraint will be obtained from the lower bounds of $\rho_t = 0.040 \text{ fm}^{-3}$ ($P_t = 0.01 \text{ MeV/fm}^3$) and it can be approximately parameterized by $R = 5.5 + 14.5M/M_\odot$ km. It is thus seen that the errors in both the transition density and pressure are still large. Thus, the uncertainties for the mass-radius relation of the Vela pulsar are still large. A conservative constraint of $R \geq 4.7 + 4.0M/M_\odot$ km using the upper bounds on the P_t and ρ_t was then obtained [9]. We notice that a constraint of $R \geq 3.6 + 3.9M/M_\odot$ km for this pulsar was previously derived in Ref. [3] by using $\rho_t = 0.075 \text{ fm}^{-3}$ and $P_t = 0.65 \text{ MeV/fm}^3$. However, the constraint obtained using data from both the terrestrial laboratory experiments and astrophysical observations is significantly more stringent.

REFERENCES

1. C. J. Pethick, D. G. Ravenhall, and C. P. Lorenz, Nucl. Phys. **A584**, 675 (1995).
2. J.M. Lattimer and M. Prakash, Phys. Rep. **333-334**, 121 (2000); Astrophys. J. **550**, 426 (2001); Science **304**, 536 (2004); Phys. Rep. **442**, 109 (2007).
3. B. Link, R. I. Epstein, and J.M. Lattimer, Phys. Rev. Lett. **83**, 3362 (1999).
4. S. B. Ruster, M. Hempel, and J. Schaffner-Bielich, Phys. Rev. C **73**, 035804 (2006).
5. B.A. Li, L.W. Chen, and C.M. Ko, Phys. Rep. **464**, 113 (2008).
6. M.B. Tsang et al., Phys. Rev. Lett. **92**, 062701 (2004).
7. L.W. Chen, C.M. Ko, and B.A. Li, Phys. Rev. Lett. **94**, 032701 (2005); Phys. Rev. C **72**, 064309 (2005).
8. B.A. Li and L.W. Chen, Phys. Rev. C **72**, 064611 (2005).
9. J. Xu, L.W. Chen, B.A. Li, and H.R. Ma, Phys. Rev. C **79**, 035802 (2009); Astrophys. J. **697**, 1549 (2009).
10. C.B. Das, S. Das Gupta, C. Gale, and B.A. Li, Phys. Rev. C **67**, 034611 (2003).
11. S. Kubis, Phys. Rev. C **76**, 035801 (2007).